Electrochemical studies of cobalt hydroxide — an additive for nickel electrodes

P. Elumalai[a], H.N. Vasan[a,*], N. Munichandraiah[b,1]

[a]*Soild State and Structural Chemistry Unit, Indian Institute of Science, Bangalore 560 012, Karnataka, India*
[b]*Department of Inorganic and Physical Chemistry, Indian Institute of Science, Bangalore 560 012, Karnataka, India*

Abstract

The electrochemical behavior of chemically precipitated cobalt hydroxide is studied by cyclic voltammetry and galvanostatic charge/discharge cycling. When cycled in the potential range between the oxygen evolution reaction (OER) and the hydrogen evolution reaction (HER), the electrode undergoes two pairs of reactions. The pair of current peaks close to the OER is attributed to quasi-reversible oxidation of $Co(OH)_2$ to $CoOOH$, whereas the pair of current peaks close to the HER is due to quasi-reversible reduction of $Co(OH)_2$ to Co. The peak current values of both reactions do not show dependence on alkali concentration. Possible mechanisms are proposed for the reactions, in which the diffusion of dissolved $Co(OH)_2$ prior to the electron-transfer step is considered to be the rate-determining step. Considering the fact that the $Co(OH)_2/CoOOH$ and $Co(OH)_2/Co$ reactions are separated by a potential difference of about 1.2 V, a galvanic cell is constructed by using two $Co(OH)_2$ electrodes in 6 M KOH. On charging, the positive electrode attained a stable potential of about 0.4 V versus Hg/HgO, OH^- and the negative electrode attained a stable potential of about -0.8 V versus Hg/HgO, OH^-, thus resulting in an open circuit cell voltage of about 1.2 V. By discharging the cell, a capacity of 15 mA h g^{-1} of $Co(OH)_2$ is obtained over about 15 charge/discharge cycles. The charged electrodes are analyzed by powder XRD and IR spectroscopy and the presence of Co and $CoOOH$ in the negative and positive electrodes, respectively, is confirmed. Although the cell is not commercially viable, the concept of a ''double hydroxide'' is demonstrated akin to the ''double sulfate'' principle of lead-acid batteries. It is expected that $Ni(OH)_2$, which is isostructural to $Co(OH)_2$, may also show a similar behavior. © 2001 Elsevier Science B.V. All rights reserved.

Keywords: Cobalt hydroxide; Cyclic voltammetry; Reaction mechanism; Oxidation to CoOOH; Reduction to Co; Galvanic cell; Double hydroxide principle

1. Introduction

Nickel hydroxide is an important electrode material. It is widely employed in several alkaline storage batteries, namely, nickel/cadmium, nickel/hydrogen and nickel/metal hydride batteries. Cobalt hydroxide is usually added for the purpose of enhancing the performance of $Ni(OH)_2$ as a battery active material [1]. Many electrochemical studies of $Ni(OH)_2$ have been reported, whereas studies of $Co(OH)_2$ are quite sparse [2–4]. Benson et al. [2] cathodically deposited $Co(OH)_2$ layers on platinum and studied the electrochemical behavior in an alkaline electrolyte by using polarization and potential-decay measurements. The results for the $Co(OH)_2$ electrode were compared with those for

$Ni(OH)_2$. Buss et al. [3] synthesized $Co(OH)_2$ and $Ni(OH)_2$, which were intercalated with $Al(OH)_2NO_3$ and studied their electrochemical properties. It was shown that $Co(OH)_2$ was charged to an oxidation state of $+3.7$ in the presence of Al. The doping of Al was, therefore, found to improve the discharge specific capacity of $Co(OH)_2$. Ismail et al. [4] cathodically deposited layers of $Co(OH)_2$ on platinum and studied their cyclic voltammetric behavior. In the present study, $Co(OH)_2$ electrodes are prepared from chemically precipitated hydroxide by pasting on current-collectors of nickel mesh. The electrodes are subjected to potentiodynamic studies in KOH electrolyte of several concentrations. The data suggest that $Co(OH)_2$ undergoes oxidation to $CoOOH$ prior to oxygen evolution, which is hitherto very well known. Additionally, $Co(OH)_2$ undergoes quasi-reversible reduction to cobalt at potentials close to the hydrogen evolution reaction. The results of cyclic voltammetry and studies of a galvanic cell based on the concept of a ''double hydroxide'' are discussed.

* Corresponding author. Tel.: +91-80-309-2951; fax: +91-80-360-1310.
E-mail addresses: vasan@sscu.iisc.ernet.in (H.N. Vasan),
muni@ipc.iisc.ernet.in (N. Munichandraiah).
¹ Co-corresponding author.

2. Experimental

Cobalt hydroxide was chemically precipitated by mixing stoichiometric quantities of 0.86 M KOH and 0.14 M $Co(NO_3)_2$. The product was washed thoroughly and dried at 80°C under vacuum. The powder X-ray diffraction (XRD) pattern of the compound matched the XRD pattern of β-$Co(OH)_2$ as reported the literature [5]. For the purpose of electrode fabrication, $Co(OH)_2$ (85 wt.%), graphite (10 wt.%) and PTFE binder (5 wt.%) were mixed and the resulting dough-like mass was spread on a pretreated, nickel mesh (10 mm × 10 mm) substrate. The electrode was pressed at 1.2 N m^{-2} for about 2 min and then heated at about 80°C overnight. The resulting electrode had a geometrical area of 1 cm^2 with a loading of about 50 mg cm^{-2} of active material. Electrochemical measurements were performed by mounting the electrode in a glass cell or a poly(propylene) container, which contained large-area Ni sheets as auxiliary electrodes. KOH electrolyte at several concentrations was prepared by dissolving AR grade KOH pellets in doubly-distilled water. The solutions were purified further by electrolyzing with large-area platinum electrodes prior to use.

Cyclic voltammetry experiments were performed by using a EG&G PARC potentiostat/galvanostat, model Versastat. The charge/discharge characteristics of the $Co(OH)_2$ electrodes were studied by means of a galvanostatic circuit which consisted of a regulated dc power source, a high resistance and an ammeter in series. Electrode potentials were measured and reported against a Hg/HgO, OH^- reference electrode by means of a digital multimeter of high input impedance. Powder XRD patterns were taken with a Co anticathode ($\lambda = 1.7902$ Å) in a JEOL JDX-8P X-ray diffractometer. Infra red spectra were attained with a Perkin-Elmer FT-IR 1000 spectrometer using a KBr pellets.

3. Results and discussion

The open-circuit potential (OCP) of the $Co(OH)_2$ electrode in a KOH electrolyte is about −0.2 V. The electrode potential was scanned starting from the OCP to encompass the oxygen evolution reaction (OER) and the hydrogen evolution reaction (HER). A typical voltammogram in 6 M KOH is shown in Fig. 1. An oxidation peak (P1) appears at 0.5 V. The increase in current subsequent to peak P1 is due to the OER. By reversing the scan at 0.8 V, a reduction peak P2 appears at about 0.3 V. Further continuation of the potential scan towards cathodic potentials results in an increase of current due to the HER at about −1.2 V. The scan direction was changed at −1.3 V to complete the potential cycle at the OCP. As seen in Fig. 1, there are no current peaks in the potential region negative to the OCP. Similar cyclic voltammetric behavior was observed at several scan rates in the range 5–200 mV s^{-1}. Although the voltammogram at positive potentials is similar to that

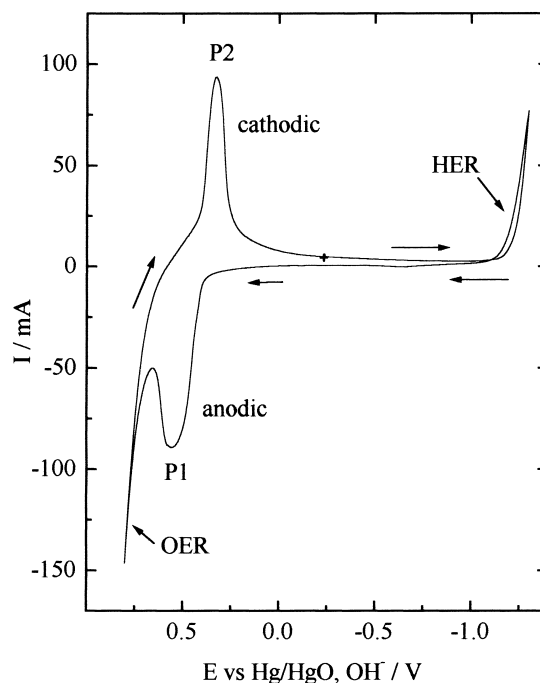Fig. 1. Cyclic voltammogram of $Co(OH)_2$ electrode (area = 1 cm^2, loading of $Co(OH)_2$ = 50 mg cm^{-2}) in 6 M KOH at a scan rate of 100 mV s^{-1}. The potential is scanned from the OCP (−0.2 V) towards the oxygen evolution reaction (OER), reversed at 0.8 V, continued up to the hydrogen evolution reaction (HER), reversed at −1.2 V, and finally reaches the OCP. P1 is the current peak for oxidation of $Co(OH)_2$ to CoOOH and P2 for reduction of CoOOH to $Co(OH)_2$.

reported for electrochemically deposited films of $Co(OH)_2$, the part at negative potentials differs slightly from the earlier study [4]. A sharp oxidation peak close to the HER and a decrease in peak current leading to final disappearance on repetition of the potential cycle has been observed by other workers [4]. The origin of this peak was not understood. In the present experiments, however, such a peak did not appear, probably because the electrode was made of chemically precipitated $Co(OH)_2$.

The peak currents (I_p) of the peaks P1 and P2 are shown as a function of $v^{1/2}$ (where v is scan rate) in Fig. 2 for the $Co(OH)_2$ electrode in 6 M KOH. A linear increase in I_p of both the peaks (P1 and P2) with $v^{1/2}$ suggests that the corresponding reactions are diffusion-controlled. The average value (0.4 V) of the peak potentials of P1 and P2 is close to the standard electrode potential of $CoOOH/Co(OH)_2$ couple (reaction 1).

$$CoOOH + H_2O + e^- = Co(OH)_2 + OH^- \qquad (1)$$
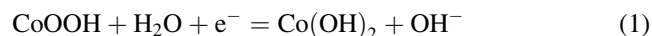
Thus, peak P1 is due to the oxidation of $Co(OH)_2$ to CoOOH and peak P2 is for the reverse process. The potential difference (ΔE_p) of the peaks is about 0.20 V and increases with scan rate (Fig. 3). The value of ΔE_p should be about 0.06 V and independent of the scan rate for a reversible, single-electron transfer process. It is, therefore, inferred that reaction (1) occurs as a quasi-reversible process during the anodic potential sweep of the $Co(OH)_2$ electrode. The quasi-
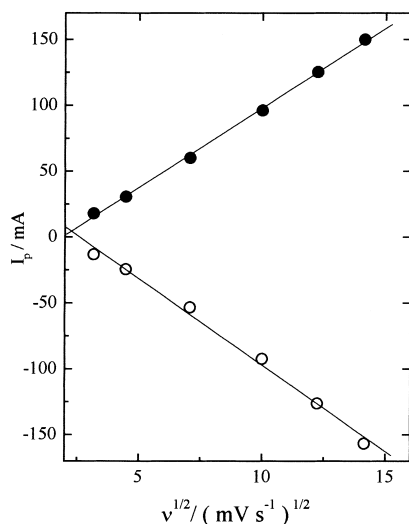
Fig. 2. Dependence of peak current (I_p) of current peak P1 ($\bigcirc$) and peak P2 ($\bullet$) on square root of scan rate (v) (area = 1 cm^2; loading of Co(OH)$_2$ = 50 mg cm^{-2}; concentration of KOH = 6 M).

reversible nature is further supported by the unequal magnitude of the charges of peaks P1 and P2. These observations are in good agreement with those made by Benson et al. [2] in polarization and potential decay studies of Co(OH)$_2$. A discharge capacity of 0.4 F mol^{-1} of Co(OH)$_2$ was obtained only when the electrode was subjected to galvanostatic charge/discharge cycles. Furthermore, it was also reported that the reduction of CoOOH to Co(OH)$_2$ did not occur at an appreciable rate although Co(OH)$_2$ was readily oxidized to CoOOH.

Potentiodynamic experiments were performed separately in the positive potential region and the negative potential region, with different starting potential values. The current peaks P1 and P2, as well as the OER currents, were
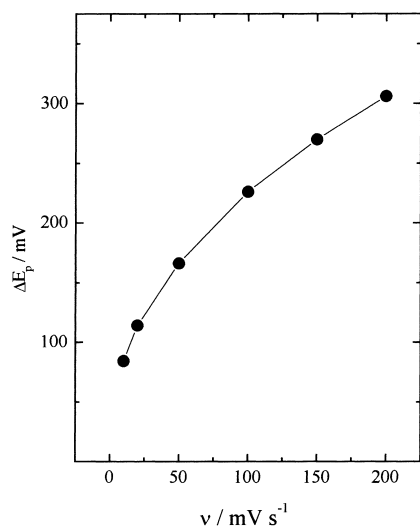

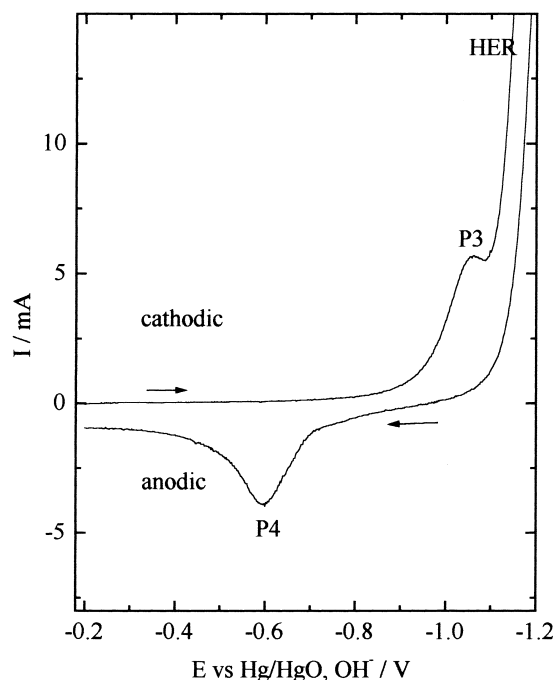Fig. 3. Dependence of peak potential difference (ΔE_p) of peaks P1 and P2 on scan rate (v).

Fig. 4. Cyclic voltammogram of Co(OH)$_2$ electrode (area = 1 cm^2, loading of Co(OH)$_2$ = 50 mg cm^{-2}) in 6 M KOH between −0.2 V and HER at a scan rate of 100 mV s^{-1}. P3 is current peak for reduction of Co(OH)$_2$ to cobalt and P4 for oxidation of cobalt to Co(OH)$_2$.

reproducible irrespective of the range of the potential scan. By contrast, the nature of the voltammogram at the negative potential region was dependent on the initial potential of the sweep. The voltammograms recorded in the potential region between −0.2 and −1.2 V (Fig. 4) showed a pair of current peaks (P3 and P4) prior to the HER. The variation of the peak current of P3 with the starting potential of the scan is shown in Fig. 5. It is interesting to note that (i) the peak current is maximum when the scan was started at −0.1 V; (ii) the peak P3 does not appear if the starting potential of the scan was positive to −0.1 V; (iii) the peak current decreases with an increase of starting potential in the negative direction (Fig. 5). The reasons for these observations are not understood at present. It is further found that the peaks P3 and P4 are present even when the scan is reversed at −0.8 V, which was well prior to the HER. It is concluded that the occurrence of peak P4 does not depend on the HER, and therefore, P4 is not due to reduction of adsorbed hydrogen on the electrode surface. Following these observations, the appearance of P3 and P4 are attributed to reaction (2), i.e.

$$Co(OH)_2 + 2e^- = Co + 2OH^- \tag{2}$$

Peak P3 is due to reduction of Co(OH)$_2$ to Co, which occurs prior to the HER. Peak P4 is, therefore, attributed to the oxidation of Co to Co(OH)$_2$ (i.e. the reverse of reaction 2). The standard electrode potential of reaction (2) is −0.63 V, which is close to the average of the peak potentials of P3 and P4. The increase in the peak currents of P3 and P4 with $v^{1/2}$ (Fig. 6) suggests that reaction (2) is controlled by diffusion.
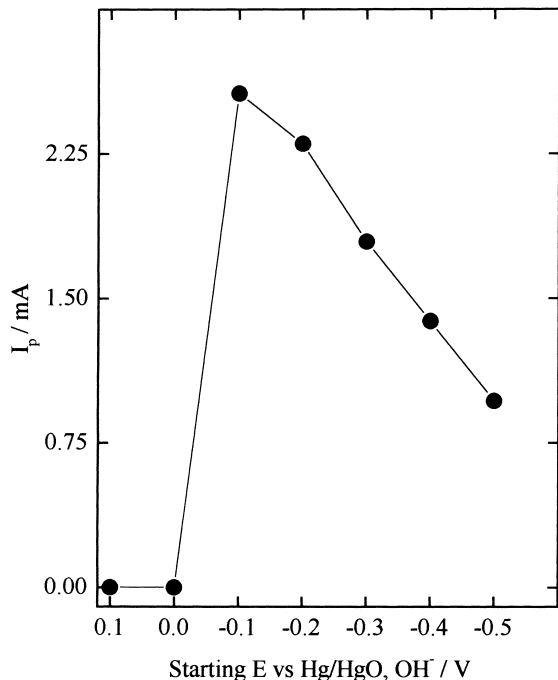
Fig. 5. Dependence of peak current of P3 of $Co(OH)_2$ electrode (area = 1 cm^2, loading of $Co(OH)_2$ = 50 mg cm^{-2}) at a scan rate of 50 mV s^{-1} in 6 M KOH on starting potential of scan.

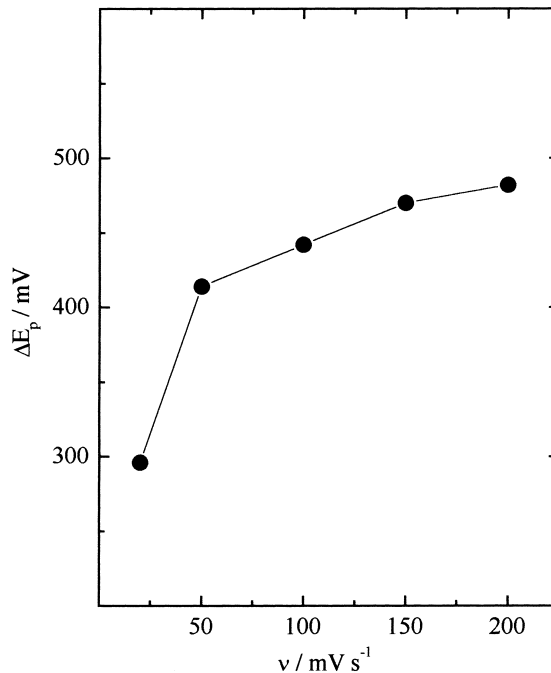Fig. 7. Dependence of peak potential difference (ΔE_p) of current peaks P3 and P4 on scan rate (v) in 6 M KOH.

The large ΔE_p and its increase with scan rate (Fig. 7) indicates that the reaction is poorly reversible.

In order to study the influence of alkali concentration on the kinetics of reactions (1) and (2), potentiodynamic experi-

ments are performed in KOH electrolytes of several concentrations in the range 0.1–6 M. The voltammograms are similar for all electrolytes. Also, the peak currents (Figs. 8 and 9) are invariant with electrolyte concentration, which
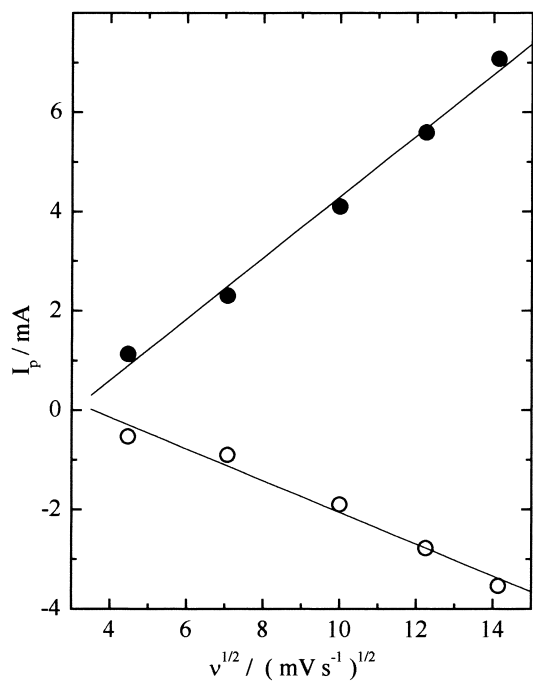

Fig. 6. Dependence of peak current (I_p) of peak P3 (●) and peak P4 (○) of $Co(OH)_2$ electrode in 6 M KOH on square root of scan rate (v) (area = 1 cm^2, loading of $Co(OH)_2$ = 50 mg cm^{-2}).
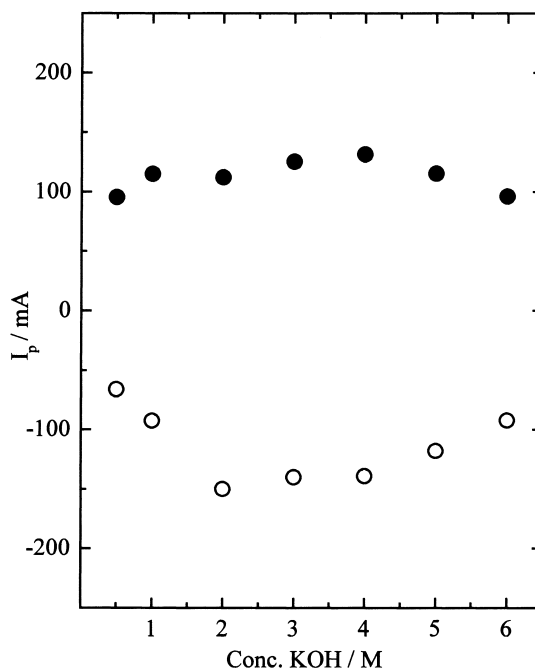

Fig. 8. Dependence of peak current (I_p) of peak P1(○) and peak P2 (●) of $Co(OH)_2$ electrode (area = 1 cm^2, loading of $Co(OH)_2$ = 50 mg cm^{-2}) on concentration of KOH electrolyte at a scan rate of 50 mV s^{-1}.

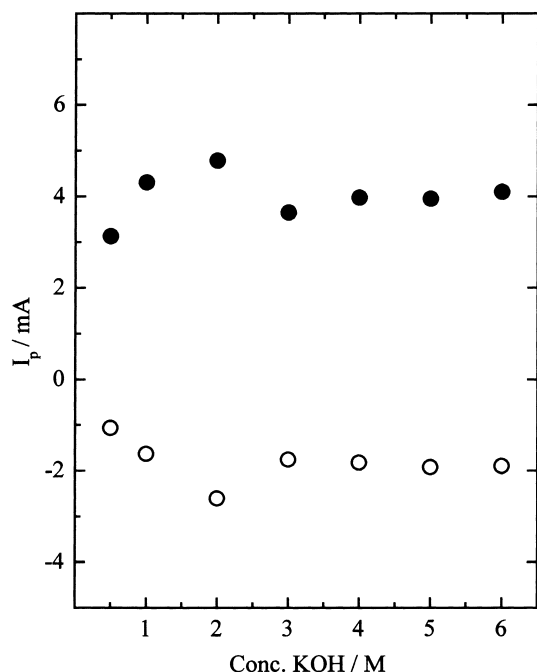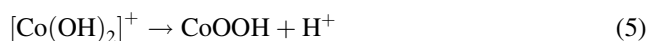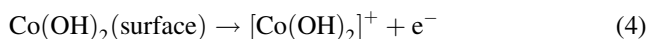Fig. 9. Dependence of peak current (I_p) of peak P3 (●) and Peak P4 (○) of $Co(OH)_2$ electrode (area = 1 cm^2, loading of $Co(OH)_2$ = 50 mg cm^{-2}) on concentration of electrolyte at a scan rate of 50 mV s^{-1}.
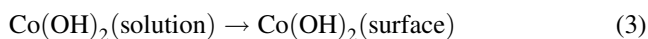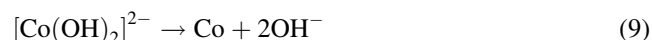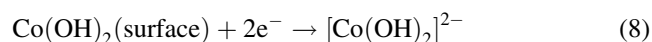
suggests that OH$^-$ ions do not influence the kinetics of reactions (1) and (2). Akin to $Ni(OH)_2$, the structure of $Co(OH)_2$ is recognized to consist of CoO^{2-} layers with protons within interlayer spaces [4]. The oxidation of $Co(OH)_2$ is considered to occur with simultaneous deprotonation to produce CoOOH (reaction 1), which indicates the influence of alkali concentration on the reaction. On the other hand, the fact that the peak currents are independent of the alkali concentration suggests that the mechanisms of these reactions consist of several sequential steps. Thus, the mechanism of reaction 1 is proposed to be

$$Co(OH)_2(\text{solution}) \rightarrow Co(OH)_2(\text{surface}) \tag{3}$$

$$Co(OH)_2(\text{surface}) \rightarrow [Co(OH)_2]^+ + e^- \tag{4}$$

$$[Co(OH)_2]^+ \rightarrow CoOOH + H^+ \tag{5}$$

$$H^+ + OH^- \rightarrow H_2O \tag{6}$$

The stoichiometric equation (reaction 1) is obtained by the addition of steps (3)–(6). It is known that $Co(OH)_2$ undergoes dissolution in alkaline electrolytes and the amount of cobalt formed from the dissolved $Co(OH)_2$ in 5 M KOH is reported to be 8 mg l^{-1} [6]. Diffusion of dissolved $Co(OH)_2$ on to the electrode surface is shown in step (3). Step (4) describes electron transfer from $Co(OH)_2$ which results in the formation of the unstable species, namely $[Co(OH)_2]^+$. A mechanism of $Co(OH)_2$ oxidation involving $[Co(OH)_2]^+$ species has been proposed by Bensen et al. [2]. Dissociation of $[Co(OH)_2]^+$ into the final oxidation product, viz. CoOOH, and a proton is shown in step (5). The proton is

converted to H_2O in alkaline electrolyte in step (6). Since the kinetics of reaction 1 are independent of KOH concentration, either step 5 or step 6 is not likely to be the rate-determination step (rds). The dependence of I_p of P1 and P2 on $v^{1/2}$ (Fig. 2) suggests that the reaction is controlled by a diffusion process, rather than by an electron-transfer process. It is concluded, therefore, that step 3 is the rate-determining step of reaction (1). In a similar way, the reduction of $Co(OH)_2$ to Co (reaction 2) is considered to proceed via

$$Co(OH)_2(\text{solution}) \rightarrow Co(OH)_2(\text{surface}) \tag{7}$$

$$Co(OH)_2(\text{surface}) + 2e^- \rightarrow [Co(OH)_2]^{2-} \tag{8}$$

$$[Co(OH)_2]^{2-} \rightarrow Co + 2OH^- \tag{9}$$

Again, the diffusion process (step 7) prior to electron-transfer step is likely to be the rate-determining step.

Considering the fact that the $Co(OH)_2$ electrode undergoes oxidation at about 0.4 V and reduction at about −0.8 V resulting in $CoOOH/Co(OH)_2$ and $Co/Co(OH)_2$ quasi-reversible couples, respectively, a combination of these reactions is expected to produce a rechargeable cell with a voltage of about 1.2 V. Two $Co(OH)_2$ electrodes were inserted into a battery container containing 6 M KOH which had provision for introducing a Hg/HgO, OH$^-$ reference electrode. Subsequent to the cell assembly, the potential value of each of the $Co(OH)_2$ electrodes was about −0.2 V, to give a cell voltage of about 0 V. The cell was subjected to charging by passing a constant current of 5 mA for about 12 h. At the end of the charging process, the open-circuit voltage of the cell attained a value of about 1.4 V with a positive electrode potential of 0.5 V and a negative electrode potential of about −0.9 V. The cell was subjected to discharge by passing a constant current of 1 mA and the discharge was continued until one of the electrodes reached −0.2 V. The charge/discharge processes were continued for about 15 cycles using a duplicate cell. A typical charge/discharge cycle and cycle-life data of the $CoOOH/Co(OH)_2//Co(OH)_2/Co$ cell are shown in Figs. 10 and 11, respectively. It is noted that the negative electrode potential remains nearly constant at about −0.8 V during the course of the cell discharge, whereas the positive electrode potential falls (Fig. 10). The decrease in cell voltage with discharge time follows the trend of positive electrode potential. A charged cell was left at open-circuit and measurements of the cell voltage and the potentials of the electrodes were made with time. The data are shown in Fig. 12. It is found that the positive electrode potential decays faster due to self discharge and, accordingly, the cell voltage decays. The decay in negative electrode potential is negligible. The data of Figs. 10 and 12 suggest that the $Co(OH)_2/Co$ reaction is more facile than the $CoOOH/Co(OH)_2$ reaction for the cell performance. It may be noted that the average capacity obtained is about 15 mA h g^{-1} of $Co(OH)_2$ (Fig. 11), which is very low in comparison with the capacity values of

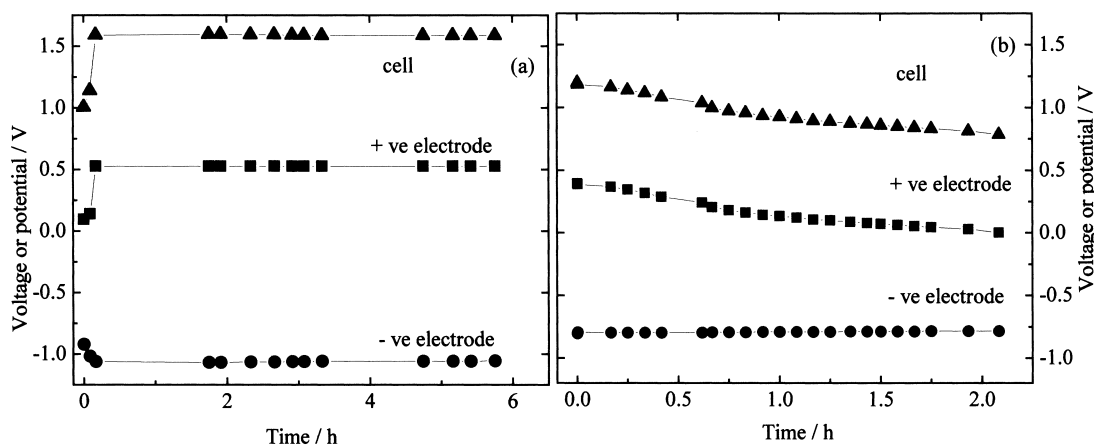Fig. 10. (a) Charge and (b) discharge curves of $CoOOH/Co(OH)_2//Co(OH)_2/CO$ cell in 6 M KOH. Electrode potentials are measured against a Hg/HgO, OH^- reference electrode. Charging current: 5 mA; discharge current: 0.5 mA (area = 1 cm^2, loading of $Co(OH)_2$ = 50 mg cm^{-2}).

commercial battery electrodes. Capacity values of about 52 mA h g^{-1} $Co(OH)_2$ are reported for the $Co(OH)_2/CoOOH$ positive electrode [3]. Enhancement of the specific capacity requires several experimental studies to determine the optimum conditions of electrode fabrication and characterization. These are not attempted in the present studies. Moreover, this type of cell has limited commercial viability due to the high cost of cobalt compounds, the solubility of $Co(OH)_2$, and the low reversibility of the electrochemical reaction. An important aspect of this study is, however, the demonstration that the quasi-reversible oxidation of $Co(OH)_2$ to $CoOOH$, on one hand, and its reduction to

Co, on the other hand, at a potential span of more than 1.2 V is conceptually useful for a battery application.

In order to substantiate the above studies, a cell assembled with two $Co(OH)_2$ electrodes was charged and the electrode materials were examined by powder X-ray diffraction (XRD). The XRD patterns of the negative and positive electrodes are shown in Fig. 13, together with the pattern of an uncharged electrode for comparison. The XRD pattern of the uncharged electrode corresponds to β-cobalt hydroxide. The XRD pattern of the negative electrode has well-defined peaks which correspond to cobalt in a mixed phase
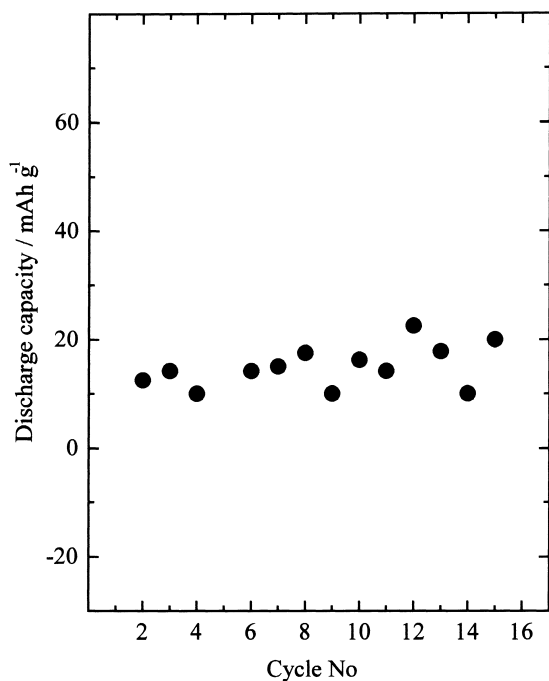

Fig. 11. Cyclic life data of $CoOOH/Co(OH)_2//Co(OH)_2/Co$ cell in 6 M KOH (area = 1 cm^2), loading of $Co(OH)_2$ = 50 mg cm^{-2}).
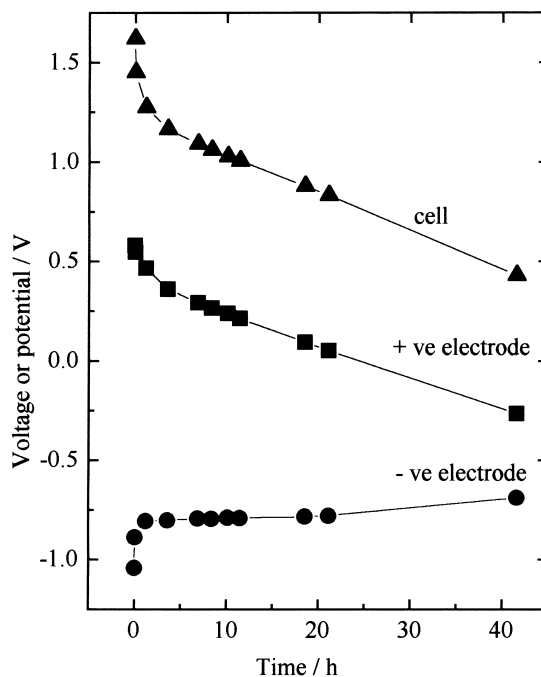
Fig. 12. Variation of electrode potentials and voltage of a charged $CoOOH/Co(OH)_2//Co(OH)_2/Co$ cell in 6 M KOH with time at open-circuit (area = 1 cm^2, loading of $Co(OH)_2$ = 50 mg cm^{-2}). Electrode potentials are measured against Hg/HgO, OH^- reference electrode.
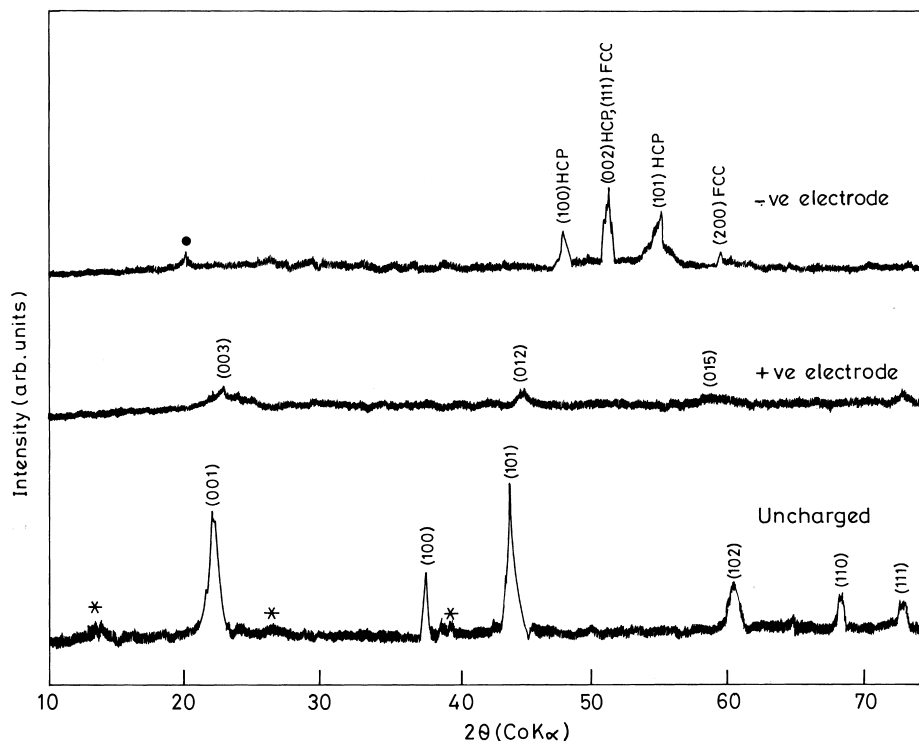
Fig. 13. Powder XRD patterns of negative electrode, positive electrode, and uncharged electrode materials: (∗) alpha phase of cobalt hydroxide; (●) graphite.

of hcp and fcc structures. It is known that cobalt is present either in an hcp phase or in a mixture of hcp and fcc phases at room temperature [7]. By contrast, the XRD of the positive electrode shows a poorly crystalline phase. The small humps present in the pattern correspond to the CoOOH of JCPDS file [8]. For a better elucidation, the positive electrode was analyzed by IR spectroscopy, which is sensitive to short-range order present in a compound. The IR spectra of the positive electrode and an uncharged electrode are shown in Fig. 14. The uncharged electrode material shows IR peaks at 3625, 485 and 435 cm^{-1} which correspond to the presence of free non-hydrogen bonded OH group and Co–O stretching frequencies, respectively. The positive electrode material exhibits a broad peak at 3100–3600 cm^{-1}, which corresponds to the presence of hydrogen bonded OH stretching frequency, and another peak at 570 cm^{-1} associated with the Co-O stretching frequency. This confirms the presence of CoOOH [9]. Furthermore, it is observed that the powder scraped from the negative electrode is attracted by a magnet, whereas the positive and uncharged powders are not attracted. The magnetic attraction of the negative electrode material is due to cobalt, which is ferromagnetic. These results confirm that on charging of the cell, the negative electrode is reduced to Co and the positive electrode is oxidized to CoOOH.

It is interesting that both the electrodes of the CoOOH/ $Co(OH)_2$//$Co(OH)_2$/Co cell are converted into $Co(OH)_2$ in the discharged state. This "double hydroxide" principle is similar to the "double sulfate" theory of the lead–acid battery in which both the positive and negative electrode

materials are converted into $PbSO_4$ in a H_2SO_4 electrolyte. Since $Co(OH)_2$ and $Ni(OH)_2$ are isostructural and their electrochemical behavior is also alike, it is anticipated that $Ni(OH)_2$ may undergo reduction to Ni in addition to its
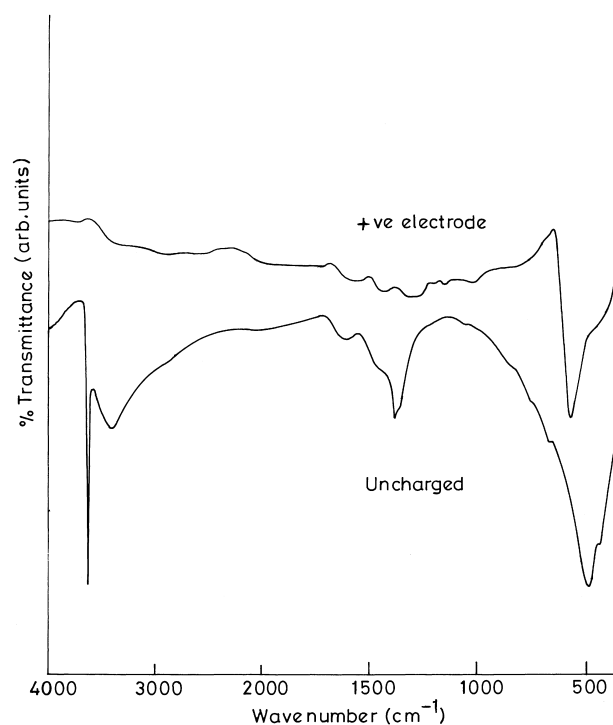

Fig. 14. IR spectra of positive electrode and uncharged electrode material.

oxidation to NiOOH. The oxidation process is well studied and exploited as the positive electrode in alkaline batteries. Based on the present studies of Co(OH)$_2$, it is anticipated that Ni(OH)$_2$ also can be used as the starting material for both the positive and negative electrodes, and such a ''all-nickel'' cell can function based on the ''double hydroxide'' principle.

4. Conclusions

A Co(OH)$_2$ electrode is found to exhibit two pairs of reactions. The pair of current peaks close to the OER is due to quasi-reversible oxidation of Co(OH)$_2$ to CoOOH, whereas the pair of current peaks close to the HER is due to quasi-reversible reduction of Co(OH)$_2$ to cobalt. The peak current values of both the reactions do not show dependence on the alkali concentration. Possible mechanisms of the reactions are proposed, in which diffusion of dissolved Co(OH)$_2$ prior to the electron-transfer step is considered to be the rate-determining step. A galvanic cell is constructed by using two Co(OH)$_2$ electrodes in 6 M KOH. The positive electrode attains a stable potential of about 0.4 V and the negative electrode attains a stable potential of about -0.8 V. This results in an open-circuit voltage of about 1.2 V subsequent upon charging. An average discharge capacity of 15 mA h g^{-1} of Co(OH)$_2$ is obtained over about 15 charge/discharge cycles. The performance of the cell is limited by the positive electrode.

References

[1] S.U. Falk, A.J. Salkind, Alkaline Storage Batteries, Wiley, New York, 1969, p. 54.
[2] P. Benson, G.W.D. Briggs, W.F.K. Wynne-jones, Electrochim. Acta 9 (1964) 281.
[3] D.H. Buss, J. Bauer, W. Diembeck, O. Glemser, J. Chem. Soc. Chem. Commun. (1985) 81.
[4] J. Ismail, M.F. Ahmed, P.V. Kamath, J. Power Sources 36 (1991) 507.
[5] JCPDS, International Center for Diffraction Data, File no. 45-0031, 1997.
[6] V. Pralong, A. Delahaye-Videal, B. Beaudoin, B. Gerand, J.-M. Tarascon, J. Mater. Chem. 9 (1999) 955.
[7] P. Elumalai, H.N. Vasan, M. Verelst, P. Lecante, V. Carles, P. Tailhades, J. Mater. Chem., submitted for publication.
[8] JCPDS, International Center for Diffraction Data, File no. 07-0169, 1997.
[9] P.V. Kamath, S. Ganguly, Mater. Lett. 10 (1991) 537.